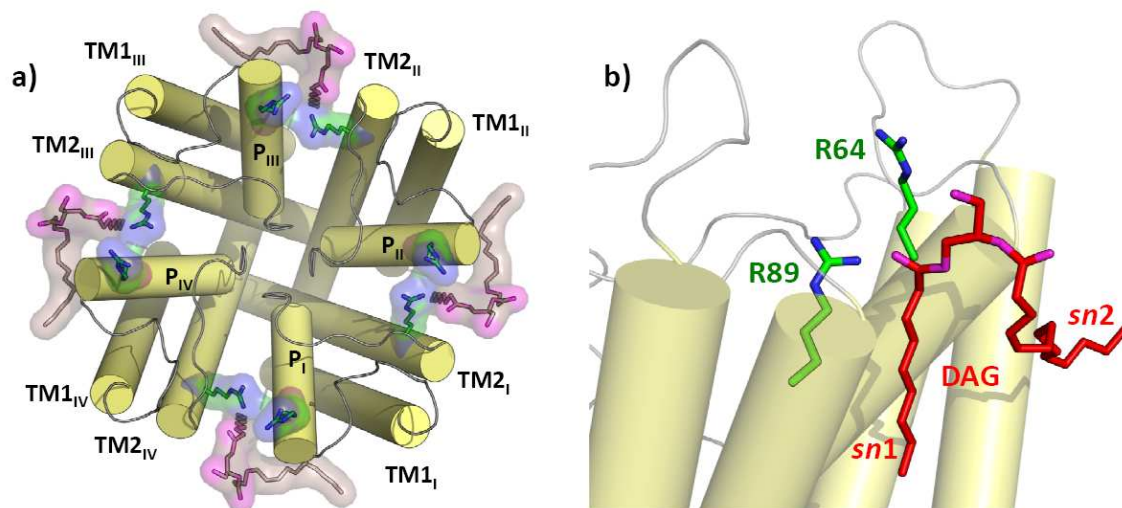


# Structural determinants of specific lipid binding to potassium channels

Markus Weingarh,<sup>†</sup> Alexander Prokofyev,<sup>†,‡</sup> Elwin A. W. van der Crujisen,<sup>†</sup> Deepak Nand,<sup>†</sup> Alexandre M. J. J. Bonvin,<sup>†</sup> Olaf Pongs,<sup>‡</sup> and Marc Baldus<sup>\*,†</sup>

*This Supporting Information contains:*

1. Figures S1 to S6
2. Details of the atomistic molecular dynamics simulations
3. References



**Figure S1.** A co-purified diacylglycerol(DAG)-fragment could be resolved with the KcsA crystal structure (PDB ID 1K4C),<sup>1</sup> the *sn1* chain of which was bound in the shallow hydrophobic groove between transmembrane helix 2 (TM2) and the pore helix (P) of two adjacent channel-subunits. The lipid-headgroup, which would be in close proximity to the positively charged residues R64 and R89, was not detected in the crystal structure.

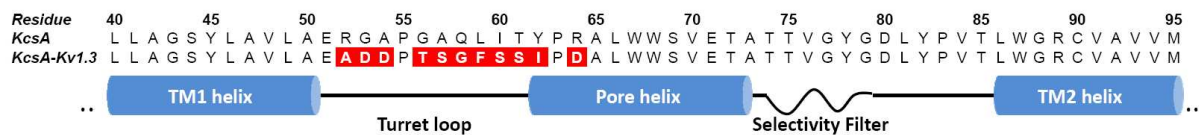


**Figure S2.** Sequence alignment of residues 40 – 95 of potassium channels KcsA and KcsA-Kv1.3. The latter is a chimeric construct<sup>2,3</sup> in which eleven residues, which are marked in red, of the S1-S2 linker of KcsA are swapped with those of the S5-S6 linker of human Kv1.3.

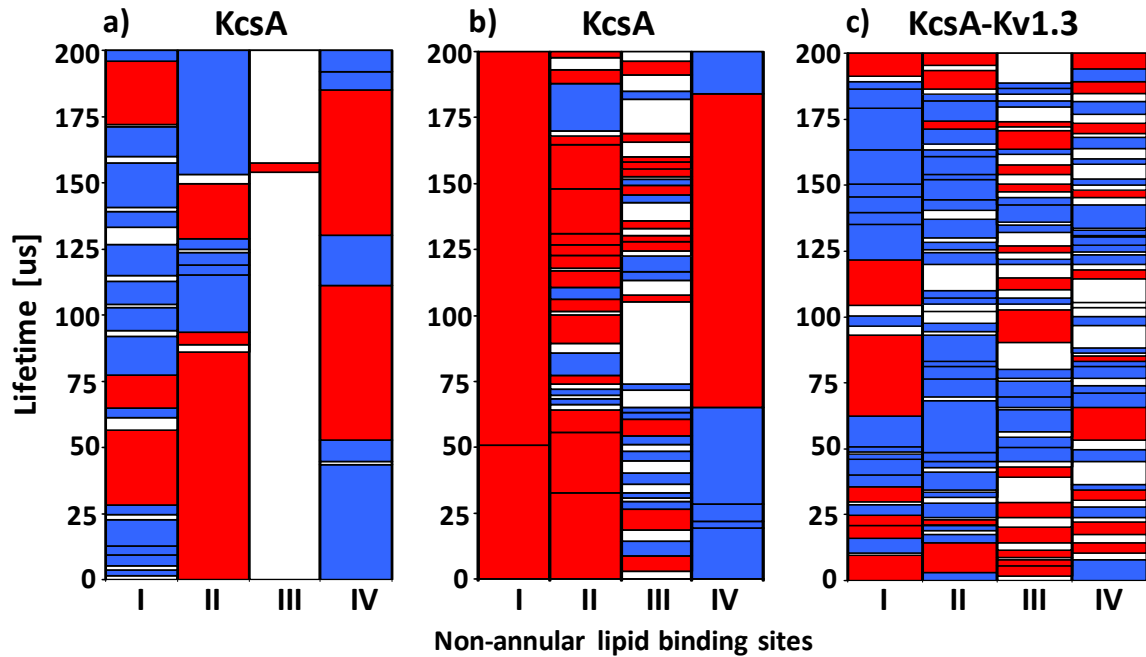


**Figure S3.** The lifetimes of DPPC (in blue) and DPPG (in red) bound to the channels' extracellular non-annular sites were established over simulations of 210  $\mu\text{s}$  (see also Figure 2 of the main text). The first 10  $\mu\text{s}$  were considered as equilibration period and discarded. To minimize the influence of the initial lipid-distribution on the lifetimes, two simulations of the same length with different initial lipid distributions were performed for KcsA (Figure S3a,b). Since the lifetimes were much shorter for KcsA-Kv1.3, the dependence on the initial lipid distribution was marginal for the chimeric channel (Figure S3c).

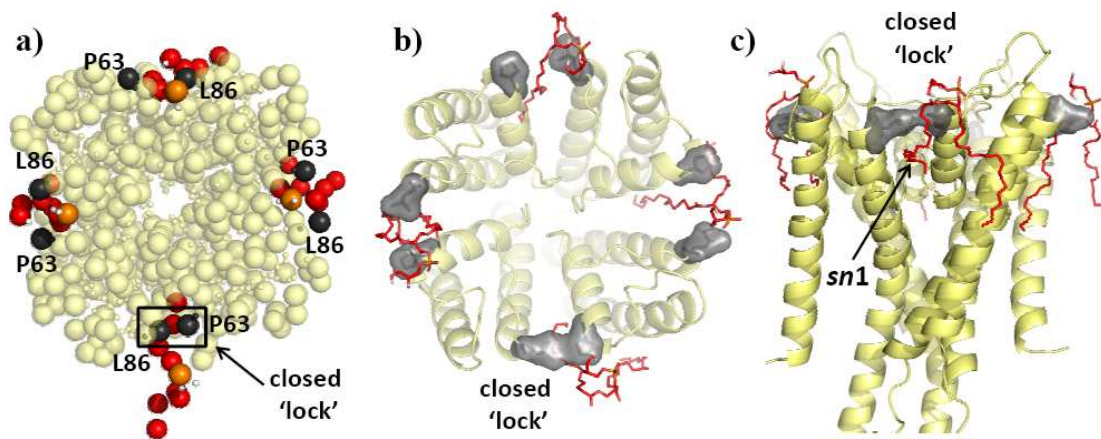


**Figure S4.** The CGMD simulations (Figures 2 of the main text and S3) showed a marked cooperativity in the non-annular lipid binding to KcsA, which matches with fluorescence and electrophysiological measurements.<sup>4</sup> In the CGMD simulations, non-annular lipid binding seems to modulate the packing of the channel-subunits with respect to each other. Residues P63 and L86 of adjacent subunits act as a kind of lock (shown as black beads), which prevents non-annular lipid-binding. Once P63 and L86 come close to each other and interact via hydrophobic forces, the non-annular site is too narrow for lipid-headgroups to bind to R64 and R89 (Figure S4a). Remarkably, this scenario could be reproduced by atomistic MD simulations in racemic POPG lipids over 60 ns (Figure S4b) (a detailed description of the setup of this simulation is given in this Supporting Information). The atomistic and CG simulations also indicate (Figure S4a,c) that the closed lock P63-L86 impedes binding of the lipid-chain to the inter-subunit hydrophobic groove.

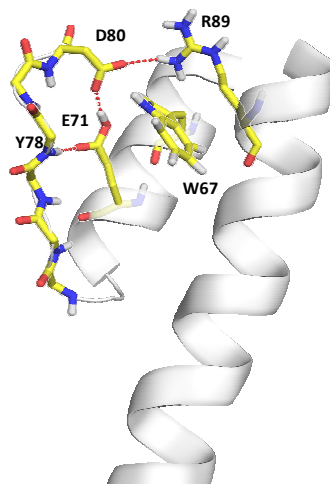


**Figure S5.** In the absence of anionic lipids, residues R64 and R89 (the latter residue is shown here) turn towards the interior of KcsA and modulate triad E71-D80-W67<sup>5-8</sup> by interacting with the carboxyl-group of D80, which in turn weakens interaction W67-D80. Since interaction W67-D80 is crucial for channel inactivation, disturbance of this interaction by interactions R64-D80 and D80-R89 may modulate the inactivation process.

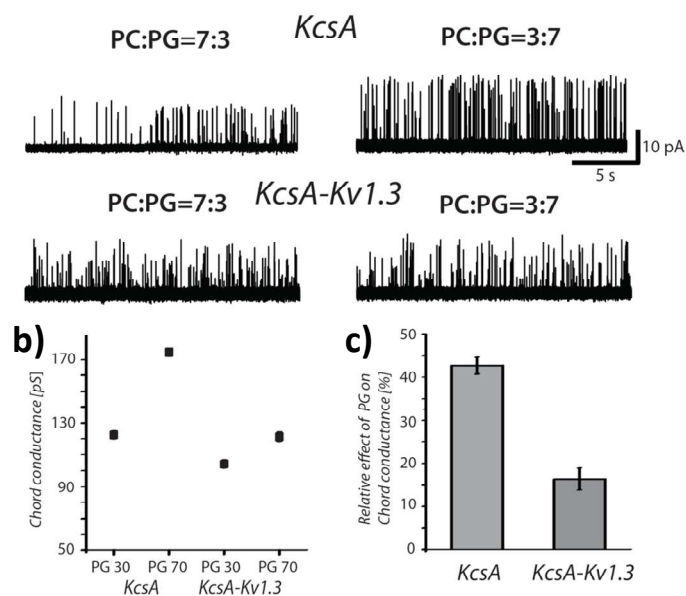


**Figure S6.** a) Representative current traces of *KcsA* and *KcsA-Kv1.3* recorded in symmetrical 150 mM KCl at +100 mV in different molar fractions of DOPG. b) Absolute and c) relative values of chord conductance of *KcsA* and *KcsA-Kv1.3* recorded in different molar fractions of DOPG.

SsNMR and CGMD data revealed strong differences in the residence time and the specificity of non-annular lipid binding to *KcsA* and *KcsA-Kv1.3*. We hypothesized that these differences, on the functional level, are correlated with different lipid sensitivities of *KcsA* and *KcsA-Kv1.3* channel activity. We tested this hypothesis using single channel measurements with varying molar ratio of anionic lipids. We found the chord conductance of *KcsA* at positive voltage significantly increased with increasing molar fraction of anionic lipids (Figure 5a-c), which matches with previous measurements<sup>4</sup>. On the other hand, the chord conductance of *KcsA-Kv1.3* changed only weakly with varying lipid composition.

## 2. Details of the atomistic molecular dynamics simulations

All simulations were carried out using the GROMACS simulations package version 4.5.3<sup>9</sup> with the GROMOS53a6 force field<sup>10</sup> and the Berger lipid parameters<sup>11</sup>. The initial coordinates and topologies of an equilibrated 128-lipid POPG bilayer and an 128 DPPC-lipid bilayer were obtained from Kukul<sup>12</sup> and Dr. Tieleman's website ([moose.bio.ucalgary.ca](http://moose.bio.ucalgary.ca)), respectively. These patches were expanded to 512 lipids, minimized, equilibrated over 10 ns and the closed-conductive KcsA channel (PDB code 3EFF)<sup>13</sup> inserted. The side chain of E71 was simulated in the protonated state<sup>7</sup>. The lipids were subsequently expanded in the transversal plane and recompressed using the inflateGRO<sup>14</sup> methodology to pack the lipids closely around the channel. For the simulation in DPPC, the channel was truncated to residues 22 – 115. The systems were subsequently solvated with SPC water and ions were added in order to neutralize the system. The final system in DPPC (105487 atoms in total) consisted of the KcsA channel, 492 lipids, 25673 water molecules, 69 potassium and 77 chloride ions, corresponding to approximately 80 mM KCl. The final system in POPG (214728 atoms in total) consisted of the KcsA channel, 497 lipids, 60782 water molecules and 497 potassium ions to electrostatically neutralize the system. In each case, three potassium ions were placed in the pore (positions S4, S2 and S0 in the selectivity filter as described in ref. <sup>7</sup>). The systems were equilibrated in an NVT-ensemble using a modified Berendsen thermostat<sup>15</sup> at 320 K (DPPC) and 310 K (POPG). Water molecules and ions were jointly coupled to the thermostat. The system was then equilibrated for 10 ns in an NPT-ensemble using the Nosé-Hoover thermostat<sup>16</sup> and semianisotropic Parrinello-Rahman pressure coupling. A production run was performed for 35 ns (DPPC) and 60 ns (POPG) with a time step of 2 fs. The PME<sup>17</sup> method was used for the long-range electrostatic forces. The LINCS algorithm<sup>18</sup> was applied to constrain the bond-lengths of the peptide and lipids and the SETTLE algorithm was used to constrain water molecules.

### 3. References

- (1) Valiyaveetil, F. I.; Zhou, Y.; MacKinnon, R. *Biochemistry* **2002**, *41*, 10771-7.
- (2) Lange, A.; Giller, K.; Hornig, S.; Martin-Eauclaire, M. F.; Pongs, O.; Becker, S.; Baldus, M. *Nature* **2006**, *440*, 959-62.
- (3) Schneider, R.; Ader, C.; Lange, A.; Giller, K.; Hornig, S.; Pongs, O.; Becker, S.; Baldus, M. *J Am Chem Soc* **2008**, *130*, 7427-35.
- (4) Marius, P.; Zagnoni, M.; Sandison, M. E.; East, J. M.; Morgan, H.; Lee, A. G. *Biophys J* **2008**, *94*, 1689-98.
- (5) Cordero-Morales, J. F.; Jogini, V.; Chakrapani, S.; Perozo, E. *Biophys J* **2011**, *100*, 2387-93.
- (6) Cuello, L. G.; Jogini, V.; Cortes, D. M.; Perozo, E. *Nature* **2010**, *466*, 203-8.
- (7) Cordero-Morales, J. F.; Jogini, V.; Lewis, A.; Vasquez, V.; Cortes, D. M.; Roux, B.; Perozo, E. *Nat Struct Mol Biol* **2007**, *14*, 1062-9.
- (8) Cordero-Morales, J. F.; Cuello, L. G.; Perozo, E. *Nat Struct Mol Biol* **2006**, *13*, 319-22.
- (9) Hess, B.; Kutzner, C.; van der Spoel, D.; Lindahl, E. *J. Chem. Theory Comput.* **2008**, *4*, 435-447.
- (10) Soares, T. A.; Hunenberger, P. H.; Kastenholtz, M. A.; Krautler, V.; Lenz, T.; Lins, R. D.; Oostenbrink, C.; van Gunsteren, W. F. *J. Comput. Chem.* **2005**, *26*, 725-737.
- (11) Berger, O.; Edholm, O.; Jahnig, F. *Biophys. J.* **1997**, *72*, 2002-2013.
- (12) Kukol, A. *J. Chem. Theory Comput.* **2009**, *5*, 615-626.
- (13) Uysal, S.; Vasquez, V.; Tereshko, V.; Esaki, K.; Fellouse, F. A.; Sidhu, S. S.; Koide, S.; Perozo, E.; Kossiakoff, A. *Proc Natl Acad Sci U S A* **2009**, *106*, 6644-9.
- (14) Kandt, C.; Ash, W. L.; Tieleman, D. P. *Methods* **2007**, *41*, 475-488.
- (15) Bussi, G.; Donadio, D.; Parrinello, M. *J. Chem. Phys.* **2007**, *126*, 014101.
- (16) Hoover, W. G. *Phys. Rev. A* **1985**, *31*, 1695-1697.
- (17) Essmann, U.; Perera, L.; Berkowitz, M. L.; Darden, T.; Lee, H.; Pedersen, L. *G. J. Chem. Phys.* **1995**, *103*, 8577-8593.
- (18) Hess, B.; Bekker, H.; Berendsen, H. J. C.; Fraaije, J. G. E. M. *J. Comput. Chem.* **1997**, *18*, 1463-1472.